Journal of Chromatography, 480 (1989) 95–110
Elsevier Science Publishers B.V., Amsterdam — Printed in The Netherlands

CHROM. 21 811

ANALYSIS OF FACTORS CAUSING PEAK BROADENING IN CAPILLARY ZONE ELECTROPHORESIS

XIAOHUA HUANG, WILLIAM F. COLEMAN[a] and RICHARD N. ZARE*
Department of Chemistry, Stanford University, Stanford, CA 94305 (U.S.A.)

SUMMARY

An equation analogous to the Van Deemter equation in chromatography is developed to account for peak broadening in capillary zone electrophoresis (CZE). This equation applies to conditions where the peaks are symmetrical (sample zone concentration much less than background electrolyte concentration). To identify and to quantitate the effects of different contributors to the peak width in CZE, it is first necessary to put all peak profiles on the same footing by correcting them for the velocities of different zones and for the finite length of the detector zone compared to the sample zone. Three major contributors to the peak width are identified: (1) the injection length of the sample; (2) longitudinal diffusion that takes place during the migration time between injection and detection; and (3) analyte–wall interactions. Temperature is shown not to be a major factor in peak broadening under typical experimental conditions. The predictions of our model agree well with experimentally determined peak profiles for different analytes under a variety of conditions. New expressions for theoretical plate number and resolution in CZE are presented. It is concluded that in almost all previously reported CZE separations the peak profiles were dominated by the sample injection length. This explains why the observed peak widths in CZE have been broader than anticipated.

INTRODUCTION

As the use of capillary zone electrophoresis (CZE) for separation and quantitation becomes more common[1–4], it is increasingly important to understand those factors that control the experimentally observed peak widths. Without this knowledge, it is not possible to establish the optimum design parameters for a CZE separation and to assess the efficacy of this new separation method compared to others.

Several models have been developed to account for peak broadening in chromatographic separations. The simplest and most commonly used of these is the so-called Van Deemter equation[5], which has been extensively tested by Katz *et al.*[6] and Jones[7]. We develop a similar equation for modeling peak broadening in CZE.

[a] Permanent address: Department of Chemistry, Wellesley College, Wellesley, MA 02181, U.S.A.

0021-9673/89/$03.50

There have been several previous studies of zone broadening in CZE. Hjertén[8], and Knox and Grant[9], as well as Grushka *et al.*[10] have considered at length the effect of temperature gradients. However, for capillary dimensions of 100 μm I.D. or less, and for currents of 30 μA or less, as is typical of most CZE separations, the effect of heat generated within the capillary tube on the separation efficiency is rather unimportant. There have been related studies by Sepaniak and Cole[11] as well as by Terabe *et al.*[12] on zone broadening in the electrokinetic chromatography of uncharged solutes, primarily with micellar solutions. The latter authors concluded that longitudinal diffusion is the dominant broadening mechanism at low velocities, while analyte–wall interactions (sorption–desorption kinetics) and heterogeneity become significant factors at higher velocities.

Separations by CZE have many of the characteristics of traditional chromatographic separations but also differ in some important aspects. Unlike chromatographic separations, different zones in CZE move past the (on-column) detector at different velocities. Because of the different residence times in the detector region, observed peak widths do not directly reflect the actual spreading of the zone in the migration channel unless an appropriate correction is applied. Additionally, the detector zone in CZE can have a length that is not negligible compared to the sample zone width. This requires another correction before the peak widths can be analyzed in terms of broadening mechanisms. Once peak widths have been properly corrected for these two effects, we model them in terms of intrinsic contributions from diffusion and analyte–wall interactions along with an extrinsic contribution from the length of the injected sample plug. This model is tested against experimental data for several different species: a positively charged, a neutral, and a negatively charged analyte. In each case, the model is able to predict successfully the observed dependence of peak width on migration time and injection length. Under certain conditions, we show that peak width measurements may be used to estimate either the diffusion constant or the length of the injected plug. Because we can model peak broadening in CZE accurately, we can design separations that have improved resolution, if desired.

EXPERIMENTAL

The experimental apparatus used in this work has been described previously[13]. Detection was accomplished either by laser-induced fluorescence (LIF)[14] or by absorption using a high-performance liquid chromatography UV spectrophotometer (UVIDEC-100-V, Japan Spectroscopic Co., Tokyo, Japan) modified for CZE detection. Both hydrostatic and electrokinetic injection were used. The capilllaries (Polymicro Technology, Phoenix, AZ, U.S.A.) in all of these studies had inside diameters of 75 μm, the distance from the injection point to the detector was between 40 and 120 cm, and voltages of 2–30 kV were applied.

The high-voltage circuitry (R50B HV power supply, Hipotronics, Brewster, NY, U.S.A.) was modified by the addition of a 80 MΩ load resistor to decrease the RC time constant (where R = resistance of electrolyte inside the capillary, and C = capacitance of circuit) of the system. This minimized the rise time and fall time of the injection voltage when electrokinetic injection was used. This is an important consideration when quantifying the size and shape of the injection plug. Fig. 1 shows the injection current obtained with and without the modification to the injection circuit described here.

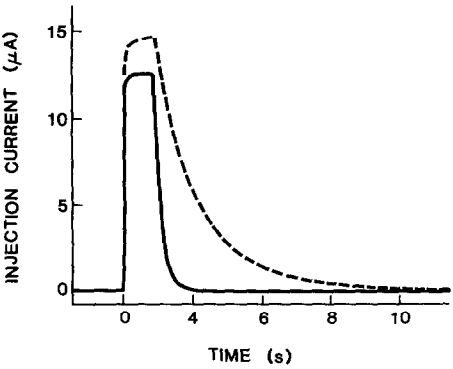

Fig. 1. Plot of injection current *vs.* time for electrokinetic injection without a load resistor in parallel to the capillary (dashed line) and with an 80 MΩ load resistor (solid line) in parallel to the capillary.

All of the compounds studied were obtained from Sigma (St. Louis, MO, U.S.A.) and were used without further purification. Samples were prepared in a buffer identical to that used as the supporting electrolyte, namely, 20 m*M* sodium phosphate at pH 7. In almost all of the experiments, the buffer concentration was at least 400 times greater than the sample concentration. Because the conductivity of the sample zones is essentially equal to that of the column as a whole, effects arising from non-uniform electric fields are minimized. Such non-uniform field effects have already been reported in CZE[8,15,16]. These effects lead to asymmetric peak broadening as well as peak narrowing caused by the fact that the leading edge of a zone migrates at a different rate than the trailing edge. To check this possibility, the peak profiles were sampled at 15 Hz, giving a time resolution of better than 0.1 s. The data are recorded using analog-to-digital conversion with the help of an IBM PC/XT computer. The peaks were then expanded up to 60 times in width and were found, in all cases, to have symmetrical profiles.

RESULTS

Correction for zone velocity

In separation methods such as liquid and gas–liquid chromatography, retention times arise from a complex series of interactions between sample molecules in the mobile phase and the components of the stationary phase and from mobile phase–solute interactions. It is generally accepted that these interactions, together with diffusion, also affect the shapes of the chromatographic peaks. Irrespective of the peak broadening mechanisms that are operative, all peaks in a given sample move past the detector region at a velocity equal to the flow velocity of the mobile phase. This flow rate depends on the back pressure of the mobile phase and any other applied driving force.

The situation is markedly different in CZE. A zone, consisting ideally of a single component of the analyte mixture surrounded by buffer, moves at a velocity that is the vector sum of the electrophoretic velocity of that component and the electroosmotic velocity of the bulk solution under the conditions of a given experiment. Thus,

molecules whose electrophoretic motion is in the same direction as the electroosmotic flow move more rapidly than neutral molecules, which in turn move more rapidly than molecules whose electrophoretic motion is in the direction opposite to the electroosmotic flow. Although it has been noted previously that different zones move at different velocities, and that this is the origin of the migration times observed in CZE[1,3,4], the effect on peak widths has not been fully appreciated.

An electropherogram obtained in a CZE experiment is a plot of the response of the detector system as a function of time. The peaks in the electropherogram, representing the various zones formed in the separation process, may be characterized by a migration time and a width. The migration time is the time required for the peak maximum to reach the detector. The full width is typically measured at the inflection point in the first derivative of the peak profile, which, for a Gaussian curve, corresponds to measuring the full width at 0.607 of the maximum height. There are alternative measurements of peak width, the most commonly encountered being the full width at half-height. For a Gaussian peak shape, the full width at half-height is 1.177 times the width defined above. In this paper, we mean by peak width the full width at the inflection point in the first derivative of the peak unless stated otherwise. We refer to this width, with units of time, as the *temporal width*.

Because the zones do not travel at the same velocity, the time required for them to pass the detector differs. This causes the temporal widths for the various zones to be unequal. Therefore, variations in temporal widths may arise solely from differences in zone velocities. It is important to realize that these different temporal widths may not imply any difference in the zone volume of the various components, or in the number of the theoretical plates for one component *versus* another.

Fig. 2a shows three Gaussian peaks, as they might appear in an electropherogram. In Fig. 2b, the widths have been corrected for differences in zone velocity, assuming an infinitely narrow (δ-function) detector, to give the actual width of the zone on the column. The correction involves simply multiplying the temporal width, w_t, by the zone velocity[17]. The zone velocity is equal to L/t_m, where L is the length of the capillary from the injection point to the detector and t_m the migration time of a particular zone. We refer to this corrected width, with units of length, as the *spatial width*. The peak height is unaffected by this velocity broadening for a δ-function, concentration-sensitive detector.

Correction for size of detection zone

In addition to the correction for zone velocity, it is also necessary to correct the peaks for the finite size of the detector region past which the zones move. It may range from several hundred microns for absorption detectors to less than 50 μm for conductivity detectors. The conversion from the temporal width of a zone, w_t, with units of time, to the spatial width of the sample in the migration channel, w_s, with units of length, is given by

$$w_s = (L/t_m)w_t - w_d \tag{1}$$

where w_d is the spatial width of the detector region. Eqn. 1 assumes that the detector response can be represented by a step function of full width, w_d. If the detector response has a more complicated dependence, then the observed widths are the convolution of the spatial width with the detector response function.

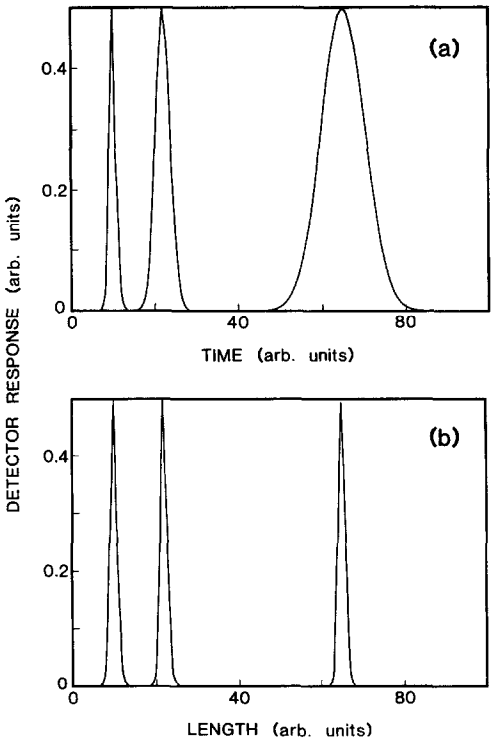

Fig. 2. Plot of detector response for three different peaks (a) as a function of time and (b) as a corresponding function of electrolyte length that has moved past the detector.

Fig. 3 shows the temporal peak widths, w_t, of dansylated lysine, run at a number of different voltages to produce different migration times, as a function of the migration time. In the same figure, we also present the conversion of those widths to spatial widths according to eqn. 1. In these experiments, the injection volume was held

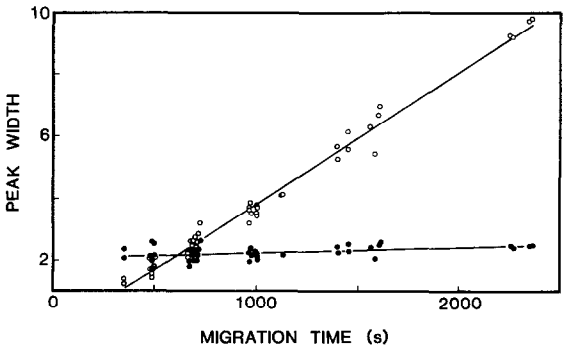

Fig. 3. Effect of correcting measured peak widths for zone velocity and detector width. The sample is dansylated lysine run at different voltages to produce different migration times. ○ = Experimentally measured (temporal) peaks (in s); ●, (spatial) peaks corrected for zone velocity and detector width (in mm). Solid lines are linear regression lines for the appropriate data set.

constant and detection was accomplished by laser-induced fluorescence. The detector zone width is approximately 75 μm. Examination of Fig. 3 shows that when the temporal widths have been corrected for velocity broadening and the finite width of the detector, all peaks in this experiment have very similar spatial widths.

We emphasize that the observed peak widths have been corrected for both velocity broadening and detector width before we assess the effect of other factors on the peak width. Unless otherwise noted, all references to peak widths in the remainder of this paper refer to spatial widths. For convenience, we refer to the spatial width of a peak as the zone length.

Peak broadening caused by diffusion and sample plug length

Several authors have assumed that one-dimensional diffusion is the major contributor to peak broadening in CZE[1,2,4]. If the sample plug that was injected were a true δ-function, that plug would spread in time, t, to a Gaussian peak with a variance equal to $2Dt$, where D is the diffusion coefficient. The zone length is equal to twice the square root of the variance, *i.e.*, $2(2Dt)^{1/2}$. This simple treatment assumes that other factors, such as heating, do not contribute to the diffusion process and that diffusion is the only broadening mechanism that is present.

The injected sample plugs are, of course, not δ-functions but have a finite width. In many experiments, we have noted zone lengths that are approximately independent of the time that a zone has spent in the column. In other cases, with smaller injection widths we find that the zone lengths do depend on the time that the samples are in the column. Thus, the extent to which diffusion affects the zone length depends on the volume of the sample plug that is injected, in particular on the *length* of the injected plug.

The total variance of a zone, once corrections have been applied for zone velocity and finite detector width, is given by

$$\sigma_{\text{tot}}^2 = \sigma_{\text{diff}}^2 + \sigma_{\text{inj}}^2 + \sigma_{\text{int}}^2 \tag{2}$$

where σ_{diff}^2 is the variance due to diffusion, $2Dt_{\text{m}}$, σ_{inj}^2 is the variance due to the injection plug length, and σ_{int}^2 represents zone-broadening variance arising from interactions between the analyte and the walls of the column. For a rectangular injection profile the variance due to injection is equal to $w_{\text{inj}}^2/12$, where w_{inj} is the width of the injected plug[18]. If the injection profile becomes non-rectangular, the expression for the variance changes. If the zone becomes trapezoidal, then the value of the denominator increases, approaching 24 as the zone profile approaches an isosceles triangle. If the observed zone shape is Gaussian, the overall width is then given by

$$w_{\text{tot}} = 2(2Dt_{\text{m}} + w_{\text{inj}}^2/12 + \sigma_{\text{int}}^2)^{1/2} \tag{3}$$

The full width at half maximum is 1.177 times this quantity.

Thus, the zone length is seen to contain contributions from an extrinsic broadening, the injection width, and two intrinsic terms, diffusional broadening and broadening caused by other interactions in the column.

Fig. 4 shows calculated zone lengths as a function of injected length for several

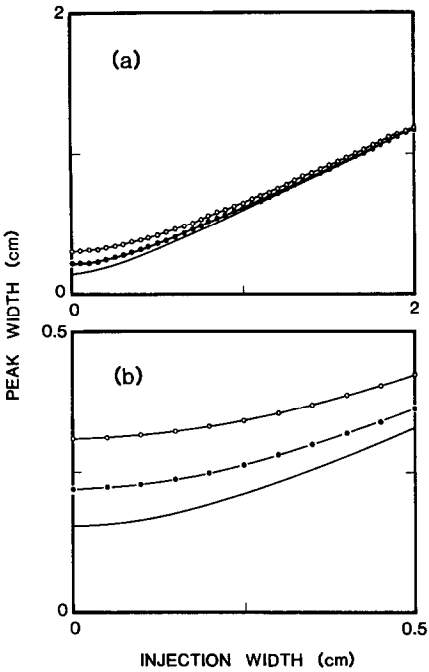

Fig. 4. Calculated peak widths as a function of injection width. Calculations are done using eqn. 3, assuming $D = 7 \cdot 10^{-6}$ cm^2/s and migration times of 300 s (line), 1200 s (●) and 2400 s (○). Trace (b) is a blow-up of (a) for short injection widths.

different migration times. The calculations are based on eqn. 3. These plots show three distinct regions:

(1) A nearly horizontal region at small injection length. In this region the zone length is determined almost exclusively by diffusion. The intercept at zero injection width is equal to $2(2Dt_m + \sigma_{int}^2)^{1/2}$. In the absence of wall interactions this expression reduces to $2(2Dt_m)^{1/2}$, the diffusion width of a δ-function injection plug.

(2) A linear region at large injection lengths. In this region and in the limit of no analyte–wall interactions the zone length becomes equal to twice the square root of the variance of the injection length. Diffusional broadening may be neglected.

(3) A region of curvature in which both diffusion and injection length contribute to the zone length.

By choosing to perform CZE experiments in region 1 it is possible to use the method to determine diffusion coefficients. By working in region 2, peak widths may provide a reliable measure of the injection volume. These conclusions are strictly valid only if broadening from analyte–wall interaction is negligible compared to the broadening from the property being measured.

Fig. 5 shows the variation of zone length with injection length for several different substances. The qualitative agreement between the experimental data and the model is quite good for injection lengths less than 0.8 cm. For each of the substances studied there is a region, at small injection lengths, where the zone length is independent of the injection length. This is followed in each case by a non-linear

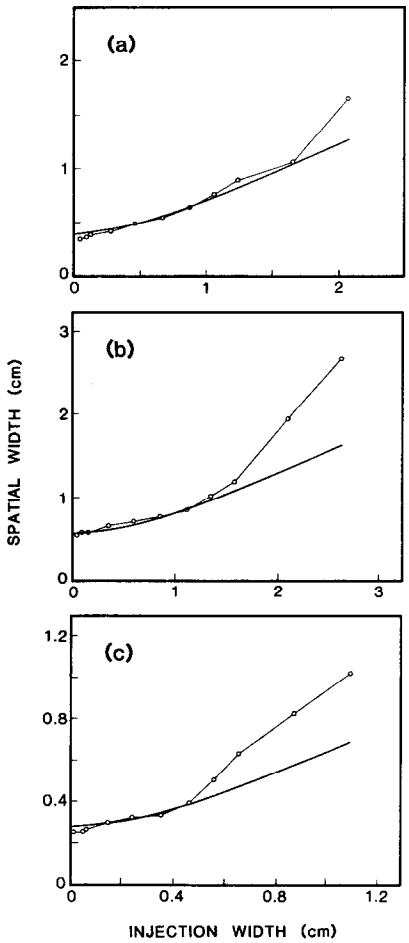

Fig. 5. The zone length as a function of the injection width for (a) adenosine, (b) adenosine monophosphate, and (c) pyroximine. Concentrations of each are $1 \cdot 10^{-5}$ *M*. The experimental data are shown by connected circles; the calculated widths, based on the parameters given in Table I and the use of eqn. 3, are shown as solid lines. Experiments were run at 20 kV. The total length of the capillary is 78 cm and the length from injection to detection is 55 cm. The buffer is 20 m*M* sodium phosphate at pH 7.

region. At large injection lengths two of the three systems show a linear dependence on injection length for injection lengths up to 2 cm.

Assuming that eqn. 2 adequately describes the experimental data, the extrapolated intercept at zero injection length may be used to calculate an effective diffusion parameter *D*. The results of these calculations are shown in Table I, together with estimates of the diffusion coefficients calculated from the Stokes–Einstein equation[19].

For two of these species, the calculated effective diffusion coefficient is significantly larger than that expected for the systems being studied. There are several reasons for this. Diffusion coefficients are directly proportional to temperature and a portion of the difference between the extrapolated diffusion coefficient and measured

TABLE I

DIFFUSION AND INTERACTION PARAMETERS

Substance	$D' \times 10^{6}$ [a]	$D_{calc} \times 10^{6}$ [b]	σ^2_{diff} [c]	σ^2_{int} [d]
Adenosine	70	9.3	0.0056	0.036
Adenosine monophosphate	16	7.2	0.0086	0.011
Pyroximine	200	9.1	0.0036	0.076

[a] From intercept in Fig. 5 and eqn. 4.
[b] From Stokes–Einstein equation.
[c] $2D_{calc}t_m$, where t_m is the migration time for each species.
[d] From eqn. 3, where σ^2_{diff} is used for $2Dt_m$.

or calculated values presumably lies in this temperature dependence. In a typical experiment, we observe that the temperature in the capillary rises approximately 12 K (from 298 to 310 K) over a period of less than 10 s for an applied voltage of 20 kV (current = 30 μA). The temperature change is directly proportional to the power, I^2R (where I = current). Such a temperature change would produce a maximum increase in the diffusion coefficient of *ca.* 35%, largely caused by the temperature dependence of the viscosity. The actual effect would be somewhat smaller, as the rate of diffusion is greatest immediately following the injection. Therefore, temperature effects alone cannot account for the differences between the effective diffusion coefficients and the diffusion coefficients of the analytes.

An effective diffusion coefficient greater than a true diffusion coefficient implies that the analyte–wall interaction term cannot be neglected under conditions where the injection length is a negligible contributor to the zone length. Table I also includes the values of the interaction variance (σ^2_{int}) that give the best fit to eqn. 3 for the species in Fig. 5. These values of σ^2_{int} should be regarded as rough approximations because of the uncertainty in the calculated diffusion coefficients.

The concept of the effective diffusion coefficient can lead to an alternative expression for the zone length

$$w_{tot} = 2(2D't_m + w^2_{inj}/12)^{1/2} \quad (4)$$

where D' is the effective diffusion coefficient. While avoiding the calculational difficulties discussed above, this approach is less instructive than that taken above for two reasons. First of all, it lumps together several effects in the effective diffusion coefficient, and secondly it implies that diffusion and these other effects have the same dependence on migration time.

It is also clear from examination of the results in Fig. 5 that with very large injection plugs, the experimental zone lengths become larger than that predicted by eqn. 3. Our treatment has assumed that the zone is Gaussian. Sternberg[18] has introduced the concept of the column as a Gaussian operator and this is indeed true up to a point. The column turns injection plugs into Gaussian zones through the action of diffusion and what we have called analyte–wall interactions. If the injected plug is too long, that process will be incomplete, resulting in a non-Gaussian zone. As the plug becomes longer, the measured peak will approach a limit where the width, as measured

from the electropherogram and corrected as described above, will approach that of the injection plug.

When a rectangular plug of finite width, h, undergoes diffusion, the concentration (c) profile is given as a function of time by

$$c(x,t) = \tfrac{1}{2}c_0\{\mathrm{erf}[h - x/2(Dt)^{1/2}] + \mathrm{erf}[x + x/2(Dt)^{1/2}]\} \quad (5)$$

where x is the position along the column, c_0 the initial concentration and erf the error function of the appropriate argument[20]. We have calculated the widths of these concentration profiles (peaks) in two ways, by explicit differentiation of eqn. 5 to find the width at the inflection point in the first derivative and by simulating the injected plug as a series of 10–100 δ-functions and numerically evaluating the width. In both cases, the resultant zone ceases to be Gaussian, and begins to have a width greater than that given by eqn. 3, when the injection width, w_{inj} in eqn. 3, is greater than 4.5–5 times the intercept of the plot of eqn. 3 *versus* injection length.

The measurement of injection length

For large injection plugs, the zone variances should be nearly equal to the variances of the injection plugs. Under these conditions, a measurement of the zone length allows an estimate of the volume of sample injected. The definition of a large injection plug depends on the migration time, or the diffusion width, of a given zone and on the distance from the injection to the detector. It also depends on negligible analyte–wall interactions. For many species, it appears that an injection plug greater than 2.5 times the diffusion width of a zone is sufficient to qualify as large. For smaller plugs, on the order of or less than the diffusion length, the situation is more complicated because plugs of varying length are seen to give rise to zones of equivalent width. For very small injection lengths the amount actually injected may be dominated by mixing at the interface between the capillary and the sample solution, and not by the contact time between the sample and the capillary hydrostatic or electrokinetic injection. We estimate that for 75-μm capillaries, the minimum injection length is approximately 200 μm. Typical injection lengths are 5–10 times larger.

Under controlled conditions, such as those used here, the concentration of the sample should have no effect on the zone length, assuming a constant injection volume. Fig. 6a shows the zone length for adenosine as a function of concentration. The zone length is seen to be independent of the concentration, depending only on the injection width. Under such conditions peak heights should be directly proportional to concentration, as is demonstrated in Fig. 6b. This observation has important implications for the use of CZE in quantitative studies.

Number of theoretical plates

Jorgenson and Lukacs[1] have given the number of theoretical plates in a CZE separation, N, as

$$N = (\mu_e + \mu_{eo})V/2D \quad (6)$$

where μ_e and μ_{eo} are the electrophoretic and electroosmotic mobilities, respectively, and V the applied voltage. They have pointed out that this expression is valid if

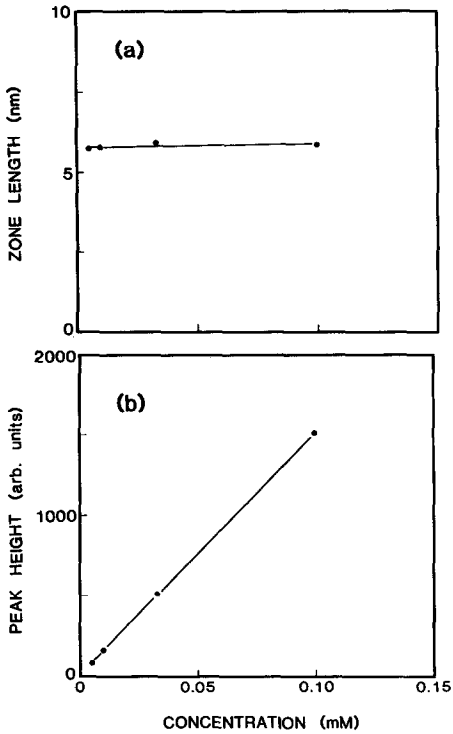

Fig. 6. Effect of adenosine concentration on (a) zone length and (b) peak height. Injection width is the same, 4.5 mm, in all cases. Experiments were run at 20 kV. The total length of the capillary is 78 cm and the length from injection to detection is 55 cm. The buffer is 20 m*M* sodium phosphate at pH 7.

diffusion is the only source of peak broadening. From eqn. 6, they inferred that separation efficiencies are enhanced for substances with small diffusion coefficients and that the number of plates increases linearly with the applied voltage. Both of these conclusions have their origin in the fact that the definition of the number of plates is

$$N = L^2/\sigma^2 \tag{7}$$

where σ^2 is the variance of the peak width (zone length). If diffusion is the only broadening mechanism then

$$\sigma = (2Dt_m)^{1/2} \tag{8}$$

where

$$t_m = L/[(\mu_e + \mu_{eo})V/l]$$

$$= Ll/[(\mu_e + \mu_{eo})V] \tag{9}$$

In eqn. 9, l is the total length of the capillary so that V/l is the electric field strength. It follows that

$$N = \frac{(\mu_e + \mu_{eo})/V}{2D}[L/l] \tag{10}$$

Only in the limit that L approaches l do we recover the formula of Jorgenson and Lukacs, eqn. 6.

As we have shown, there appear to be few, if any, situations in which the zone length is controlled by diffusion alone! At small injection lengths, the zone length is controlled by diffusion and what we have called wall interactions, while at larger injection lengths the zone length is almost completely determined by the variance of the injected plug. Thus, an expression for N must involve the total spatial variance of the zone as follows:

$$N = L^2/(\sigma^2_{diff} + \sigma^2_{inj} + \sigma^2_{int}) \tag{11}$$

from which it follows that

$$N = \frac{L^2}{\left[\frac{2DLl}{(\mu_e + \mu_{eo})V} + \frac{w^2_{inj}}{12} + \sigma^2_{int}\right]} \tag{12}$$

In almost all previous experiments, the injection plug length was large relative to the diffusion length, $2(2Dt_m)^{1/2}$. For example, in the work of Wallingford and Ewing[21] on separations in 12.6-μm capillaries, the reported injection volume of 430 pl yields an injection length of 3.5 mm, approximately 2.3 times the diffusion width for the observed migration time. In such situations, the expression for N approaches

$$N = 12L^2/w^2_{inj} \tag{13}$$

Thus, in CZE, the number of theoretical plates varies linearly with the applied voltage only in the case of very small injection lengths. Even in that instance, the expression for N still contains the term in σ^2_{int}. In the more common case, where eqn. 13 is applicable, N depends on sample concentration and on the total amount of sample only as those quantities are reflected in the injection plug length. In this limit, and in the absence of additional interactions that influence the zone length, the number of plates is the same for each component of the mixture. Again, we emphasize that it is the plug length, not the plug volume, that is important in determining the zone length. This explains the observations by Tsuda *et al.*[22] that N is not proportional to V in their careful studies. Fig. 7 shows the number of plates for adenosine as a function of applied voltage, V, and length of the capillary from injection to detection, L. The essentially complete lack of dependence of N on V and the quadratic dependence of N on L imply that eqn. 13, rather than eqn. 6 or eqn. 12, describes the plate number in these experiments.

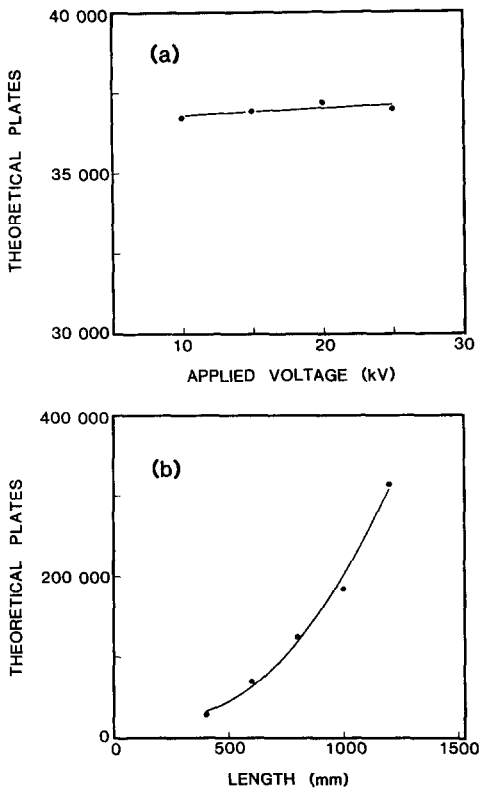

Fig. 7. Dependence of theoretical plate number, N, on (a) applied voltage, V, and (b) capillary length from injection to detection, L. The sample is adenosine and the same injection width, 4.5 mm, is used in all cases. In (a) the capillary length is 78 cm overall and 55 cm from injection to detector. In (b) the applied electric field is 200 V/cm and the length of the capillary between injection and detection is varied. The buffer is 20 mM sodium phosphate at pH 7.

Resolution

Often a more useful index for assessing the performance of a CZE separation is the resolution, R, between two zones 1 and 2, which is defined as

$$R = 1/4\ N^{1/2}\ (\Delta v/v)$$

$$= 1/2\ N^{1/2}\ [(|\ v_2 - v_1|)/(v_2 + v_1)] \tag{14}$$

where N is the average number of theoretical plates, Δv is the absolute difference in the zone velocities, v is the average zone velocity and v_1 and v_2 are the velocities of the two zones in question[23]. Using eqn. 12 we can express R as

$$R = (L/2)\frac{|(v_2 - v_1)|\ /(v_2 + v_1)}{\left[\dfrac{2DLl}{(\mu_e + \mu_{eo})V} + \dfrac{w_{inj}^2}{12} + \sigma_{int}^2\right]^{1/2}} \tag{15}$$

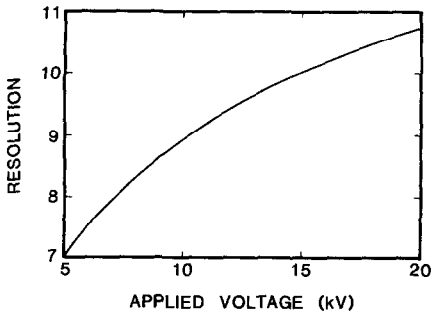

Fig. 8. Dependence of resolution, R, on applied voltage, V, according to eqn. 15. The calculation is for the resolution between two species that have the same electroosmotic mobility ($3.0 \cdot 10^{-4}$ cm^2 V^{-1} s^{-1}) and electrophoretic mobilities of 3.0 and $3.15 \cdot 10^{-4}$ cm^2 V^{-1} s^{-1}. The diffusion coefficient is that of adenosine. The injection width is set at 4.5 mm and the wall interaction term is set equal to zero. The capillary parameters are those from Fig. 7a.

This expression leads to the voltage dependence shown in Fig. 8. It is important to note that voltage influences resolution only in the case of small injection volumes, as shown in Fig. 9.

Fig. 10 shows the number of plates as a function of the injection plug at 20 kV and an analyte–wall interaction comparable to that observed experimentally for adenosine. Again, the analyte–wall interaction is only important at small injection lengths.

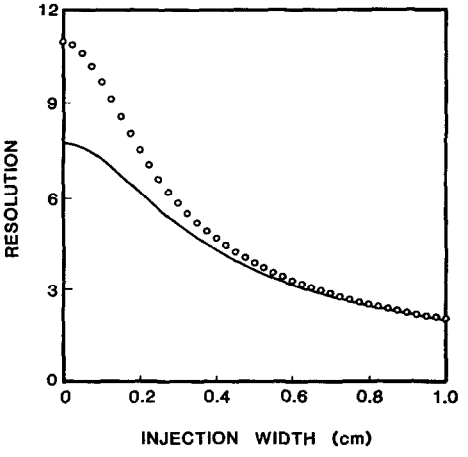

Fig. 9. Dependence of resolution, R, on injection width at two different applied voltages: 10 kV (line) and 20 kV (○). This plot is calculated from eqn. 15 using appropriate parameters from Fig. 8.

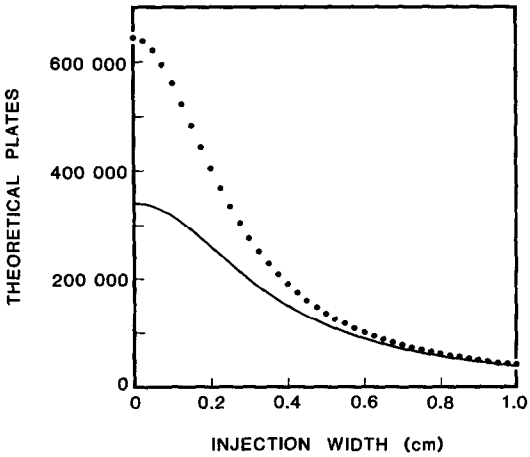

Fig. 10. Dependence of theoretical plate number, N, on injection width for no analyte–wall interaction (●) and for analyte–wall interaction (solid line) appropriate for adenosine (see Table I). Applied voltage is assumed to be 20 kV.

CONCLUSION

We have developed a model for spatial peak widths (zone lengths) in CZE that is similar in nature, but quite different in specifics, to the Van Deemter equation. This model will be useful in designing CZE experiments, particularly in cases where the method is to obtain improved quantitation or to improve resolution. The model was developed neglecting effects of heating and electrical distortions. It is expected to become more valid as the concentration of the species in the zones decreases, as this situation minimizes the effects that arise from differences in electrical properties between the zones and the background electrolyte in the migration channel.

We have shown that the length of the injection plug is often the most significant factor in determining the lengths of the individual zones in CZE under typical experimental conditions. As long as the injection length is several times the diffusion length for the species in the zone, the observed zone lengths will be approximately equal to the injection length divided by the square root of 3, *i.e.*, $w_{tot} = w_{inj}/3^{1/2}$. Although such operating conditions do not produce the largest number of theoretical plates, the number of plates is the same for each zone. In addition, quantitation should be easier with larger injection lengths. An understanding of the mechanisms for peak broadening in CZE defines the practical tradeoff between improved sensitivity and improved resolution.

ACKNOWLEDGEMENTS

We thank S. L. Pentoney, Jr., M. A. Roach and M. J. Gordon for many useful discussions. This work was supported in part by Beckman Instruments, Inc. WFC acknowledges Wellesley College and NSF grant CHE-85-05926 for sabbatical leave support.

REFERENCES

1 J. W. Jorgenson and K. D. Lukacs, *Science (Washington, D.C.)*, 222 (1983) 266.
2 A. G. Ewing, R. A. Wallingford and T. M. Olefirowicz, *Anal. Chem.*, 61 (1989) 292A.
3 M. J. Gordon, X. Huang, S. J. Pentoney, Jr. and R. N. Zare, *Science (Washington, D.C.)*, 242 (1988) 224.
4 R. A. Wallingford and A. G. Ewing, *Adv. Chromatogr.*, in press.
5 J. J. van Deemter, F. J. Zuiderweg and A. Klinkenberg, *Chem. Eng. Sci.*, 5 (1956) 271.
6 E. Katz, K. Ogan and R. P. W. Scott, *J. Chromatogr.*, 270 (1983) 51.
7 W. L. Jones, *Anal. Chem.*, 33 (1961) 829.
8 S. Hjertén, *Chromatogr. Rev.*, 9 (1967) 122.
9 J. H. Knox and I. H. Grant, *Chromatographia*, 24 (1987) 135.
10 E. Grushka, R. M. McCormick and J. J. Kirkland, *Anal. Chem.*, 61 (1989) 241.
11 M. J. Sepaniak and R. O. Cole, *Anal. Chem.*, 59 (1987) 472.
12 S. Terabe, K. Otsuka and T. Ando, *Anal. Chem.*, 61 (1988) 251.
13 E. Gassmann, J. E. Kuo and R. N. Zare, *Science (Washington, D.C.)*, 230 (1985) 813.
14 P. Gozel, E. Gassmann, H. Michelsen and R. N. Zare, *Anal. Chem.*, 59 (1987) 44.
15 F. E. P. Mikkers, F. M. Everaerts and Th. P. E. M. Verheggen, *J. Chromatogr.*, 169 (1979) 11.
16 S. Hjertén, in G. Milazzo (Editor), *Topics in Bioelectrochemistry and Bioenergetics*, Vol. 2, Wiley, New York, 1978, pp. 89–128.
17 S. Hjertén, K. Elenbring, F. Kilár, Jia-Li Liao, A. J. C. Chress, C. J. Sierbert and M.-D. Zhu, *J. Chromatogr.*, 403 (1987) 47.
18 J. C. Sternberg, *Adv. Chromatogr.*, 2 (1966) 206–270.
19 R. A. Robinson and R. H. Stokes, *Electrolyte Solutions*, Academic Press, New York, 1959.
20 J. Crank, *The Mathematics of Diffusion*, Oxford University Press, New York, 2nd ed., 1975.
21 R. A. Wallingford and A. G. Ewing, *Anal. Chem.*, 60 (1988) 1972.
22 T. Tsuda, G. Nakagawa, M. Sato and K. J. Yagi, *Appl. Biochem.*, 5 (1983) 330.
23 J. C. Giddings, *Sep. Sci.*, 4 (1969) 181.